Small-signal analysis of the Boltzmann equation from harmonic- and impulse-response methods

J. C. Vaissiere, J. P. Nougier, L. Varani,* and P. Houlet
Centre d'Electronique de Montpellier, Université Montpellier II, 34095 Montpellier CEDEX 5, France

L. Hlou
Faculté des Sciences de Kénitra, Kénitra, Morocco

E. Starikov and P. Shiktorov
Semiconductor Physics Institute, Goshtauto 11, 2600 Vilnius, Lithuania

L. Reggiani
Dipartimento di Fisica, Università di Modena, Via Campi 213/A, 41100 Modena, Italy
(Received 26 October 1993)

We present two original methods which yield the small-signal response around the dc bias in bulk semiconductors, using direct numerical resolutions of the perturbed Boltzmann equation. The first method operates in the frequency domain. An ac sinusoidal electric-field perturbation superimposed to the dc field produces an ac perturbation of the distribution function which is computed at each frequency. The second method operates in the time domain. A step electric-field perturbation is superimposed at time $t=0$ to the dc field. The resulting perturbations of the distribution function and of the average velocity are then computed as functions of time. These methods are applied to the case of holes in silicon at $T=300$ K under hot-carrier conditions and are used to compute the perturbed distribution function and the differential mobility spectrum.

I. INTRODUCTION

Modern microelectronics is evolving toward a deep miniaturization (submicron scale length) and a search to increase the operation frequency of semiconductor devices (terahertz frequency range). As a consequence, the knowledge of small-signal kinetic coefficients (e.g., differential mobility, impedance, admittance, current spectral-density, etc.) is of relevant importance to model and forecast device performances. From a microscopic point of view, a proper modeling should account for several physical phenomena, such as velocity overshoot, carrier heating, intervalley transfer, etc., which are inherent to the space and time scales mentioned above.

To date the most comprehensive theoretical analysis of these phenomena is based on numerical solutions of the Boltzmann equation (BE). For this purpose, the ensemble Monte Carlo (MC) technique has emerged as a very powerful method, because of its capability to include many details of the model without introducing approximations in solving the BE.[1-6] However, together with evident advantages, the MC technique also has inherent shortcomings mainly related to the stochastic nature of the procedure. Typically, the standard MC scheme[1,4] meets with difficulties in calculating with high accuracy quantities on a hydrodynamic time scale, such as the small-signal coefficients, rare events, space profile and transient evolution of the free-carrier concentration, average velocity, average energy, etc. To overcome these difficulties some refined procedures such as the Price perturbative algorithm,[7] direct simulation of the distribution function gradient in momentum space,[8] weighted MC method,[9] etc. have been developed. However, as a rule, these procedures significantly increase the complexity of MC codes without removing completely the cited difficulties. Therefore, in recent years some efforts have been made to develop various deterministic (as opposite to stochastic) methods of solving the BE in bulk semiconductors and semiconductor devices.[10-21] Most of these methods deal with the steady-state hot-carrier transport, and often cannot be reformulated in terms of the time-dependent BE. However, the direct solution of the transient transport is of great interest since it can provide the spectral dependence of the small-signal kinetic coefficients in bulk semiconductors as well as in semiconductor devices.

Linear-response functions around the bias point are known to play a fundamental role in the investigation of hot-carrier transport and noise in bulk semiconductors.[7,16,21-29] In the time domain they reflect both dynamic and relaxation processes inherent to the hot-carrier system, and can be used for the detailed investigation of kinetic phenomena. In the frequency domain they provide the differential (ac) mobility spectrum necessary to evaluate a possibility of amplification and generation, to calculate the gain or the absorption coefficients, to obtain the noise temperature using the spectral density of velocity fluctuations, etc.

The aim of this paper is to present two deterministic approaches which enable us to obtain the ac characteristic of bulk semiconductors around the dc bias point, so as to obtain the ac mobility which is of great interest since it can be measured experimentally. The methods are based on a direct solution of the transient BE in the frequency

and time domains, and, for validation purpose, are applied to the case of holes in silicon at $T=300$ K.

The content of the paper is organized as follows. In Sec. II the small-signal BE is given. The method for computing the harmonic response is explained in Sec. III. The impulse method is studied in Sec. IV. The results of the calculations, as applied to the case of holes in Si, are summarized in Sec. V. Finally some conclusions are given in Sec. VI.

II. SMALL-SIGNAL TRANSPORT AND DISTRIBUTION FUNCTION

The distribution function $f(\mathbf{k},t)$ of carriers in homogeneous nondegenerate semiconductors with a uniform external applied electric field $\mathbf{E}(t)$ is the solution of the time-dependent BE:

$$\frac{\partial f(\mathbf{k},t)}{\partial t}+\frac{e\mathbf{E}(t)}{\hbar}\cdot\nabla_{\mathbf{k}}f(\mathbf{k},t)=Cf(\mathbf{k},t)\ ,$$

$$Cf(\mathbf{k},t)=\frac{1}{(2\pi)^3}\int P(\mathbf{k}',\mathbf{k})f(\mathbf{k}',t)d^3k'-\frac{f(\mathbf{k},t)}{\tau(\mathbf{k})}\ , \tag{1}$$

$$\frac{1}{\tau(\mathbf{k})}=\frac{1}{(2\pi)^3}\int P(\mathbf{k}',\mathbf{k})d^3k'\ ,$$

with the proper initial conditions.

In Eq. (1), the term $P(\mathbf{k}',\mathbf{k})$ is the sum of all the transition rates $W_i(\mathbf{k}',\mathbf{k})$ from state $\mathbf{k}'$ to state $\mathbf{k}$ associated with the scattering mechanism number i. Integrals in Eq. (1) extend over the whole $\{\mathbf{k}\}$ space. By further integrating Eq. (1) over the whole $\{\mathbf{k}\}$ space, in the absence of generation recombination terms, one readily obtains

$$\frac{\partial\int f(\mathbf{k},t)d^3k}{\partial t}=0\ . \tag{2}$$

The average value $\varphi(t)$ of any function $\varphi(\mathbf{k})$ of state $\mathbf{k}$ is given by

$$\varphi(t)=\left[\int\varphi(\mathbf{k})f(\mathbf{k},t)d^3k\right]\left[\int f(\mathbf{k},t)d^3k\right]^{-1}\ . \tag{3}$$

In particular, the average velocity $\mathbf{v}(t)$ is given at any time by

$$\mathbf{v}(t)=\left[\int\mathbf{v}(\mathbf{k})f(\mathbf{k},t)d^3k\right]\left[\int f(\mathbf{k},t)d^3k\right]^{-1}\ , \tag{4}$$

where $\mathbf{v}(\mathbf{k})=(1/\hbar)\nabla_{\mathbf{k}}\varepsilon(\mathbf{k})$, $\varepsilon(\mathbf{k})$ being the energy-wave-vector relationship.

In a constant electric field $\mathbf{E}_S$ of magnitude E_S $f(\mathbf{k},t)$ takes the stationary value

$$f_S(\mathbf{k})\equiv f_S(\mathbf{k},\mathbf{E}_S)=\lim_{t\to\infty}f(\mathbf{k},t)\ ,$$

where $f_S(\mathbf{k})$ is the solution of the stationary BE:

$$\frac{e\mathbf{E}}{\hbar}\cdot\nabla_{\mathbf{k}}f_S(\mathbf{k})=Cf_S(\mathbf{k})\ . \tag{5}$$

Analogously, the stationary velocity $\mathbf{v}_S$ is given by Eq. (4), where $f(\mathbf{k},t)$ has to be replaced by $f_S(\mathbf{k})$:

$$\mathbf{v}_S=\left[\int\mathbf{v}(\mathbf{k})f_S(\mathbf{k})d^3k\right]\left[\int f_S(\mathbf{k})d^3k\right]^{-1}\ . \tag{6}$$

Now, if a small electric field $\delta\mathbf{E}(t)$ is superimposed on $\mathbf{E}_S$, this produces a variation of the distribution function $\delta f(\mathbf{k},t)$, obtained by setting, in Eq. (1),

$$\mathbf{E}(t)=\mathbf{E}_S+\delta\mathbf{E}(t)\ \text{ and }\ f(\mathbf{k},t)=f_S(\mathbf{k})+\delta f(\mathbf{k},t)\ .$$

By expanding Eq. (1), the zero-order terms give Eq. (5), and the first-order terms give $\delta f(\mathbf{k},t)$ as a solution of

$$\frac{\partial}{\partial t}\delta f(\mathbf{k},t)+\frac{e\mathbf{E}_S}{\hbar}\cdot\nabla_k\delta f(\mathbf{k},t)-C\delta f(\mathbf{k},t)=-\frac{e\delta\mathbf{E}(t)}{\hbar}\cdot\nabla_{\mathbf{k}}f_S(\mathbf{k})\ . \tag{7}$$

The average velocity becomes $\mathbf{v}(t)=\mathbf{v}_S+\delta\mathbf{v}(t)$, where the small-signal velocity $\delta\mathbf{v}(t)$ is obtained by expanding Eq. (4) to first order, which, taking into account Eqs. (2) and (6), gives

$$\delta\mathbf{v}(t)=\left[\int\mathbf{v}(\mathbf{k})\delta f(\mathbf{k},t)d^3k\right]\left[\int f_S(\mathbf{k})d^3k\right]^{-1}\ . \tag{8}$$

III. HARMONIC-RESPONSE METHOD

A. Definitions

When the perturbation is sinusoidal, the response is also sinusoidal. That is, if

$$\delta\mathbf{E}_{\text{har}}(t)=\delta\mathbf{E}\exp(i\omega t)$$

then (9)

$$\delta f(\mathbf{k},t)=\delta f(\mathbf{k},\omega)\exp(i\omega t)\ ,$$

and these quantities substituted into Eq. (7) give $\delta f(\mathbf{k},\omega)$ as a solution[30] of

$$i\omega\delta f(\mathbf{k},\omega)+\frac{e\mathbf{E}_S}{\hbar}\cdot\nabla_{\mathbf{k}}\delta f(\mathbf{k},\omega)-C\delta f(\mathbf{k},\omega)=-\frac{e\delta\mathbf{E}}{\hbar}\cdot\nabla_{\mathbf{k}}f_S(\mathbf{k})\ . \tag{10}$$

Equation (8) shows that $\delta\mathbf{v}(t)=\delta\mathbf{v}(\omega)\exp(i\omega t)$, where $\delta\mathbf{v}(\omega)$ is given by

$$\delta\mathbf{v}(\omega)=\left[\int\mathbf{v}(\mathbf{k})\delta f(\mathbf{k},\omega)d^3k\right]\left[\int f_S(\mathbf{k})d^3k\right]^{-1}\ . \tag{11}$$

The complex quantities $\delta\mathbf{v}(\omega)$ and $\delta\mathbf{E}$ are linearly related through $\mu(\omega)$, the ac mobility tensor at frequency ω depending on $\mathbf{E}_S$ as

$$\delta\mathbf{v}(\omega)=[\mu(\omega,\mathbf{E}_S)]\delta\mathbf{E}\ . \tag{12}$$

B. Calculations

By assuming a spherical symmetry of the band model, the perturbation term $\delta f(\mathbf{k},\omega)$ can be written $\delta f(k,\theta,\omega)$, where $k=|\mathbf{k}|$ and $\theta=(\mathbf{E},\mathbf{k})$. The same mesh in $\{\mathbf{k}\}$ space is then used to discretize Eq. (10) and compute $f_S(k,\theta)$. After discretization, the gradient and the collision operators appear as linear combinations of $\delta f(k_i,\theta_j,\omega)$; hence Eq. (10) at any $\{k_i,\theta_j\}$ can be written as

$$\sum_{l,m}a_{l,m}\delta f(k_l,\theta_m,\omega)=-\frac{e\delta\mathbf{E}}{\hbar}\cdot\frac{\partial f_S(\mathbf{k})}{\partial\mathbf{k}_z}\ , \tag{13}$$

where the $a_{l,m}$ are complex coefficients which depend on the discretization procedure (such as central difference schemes to express the collision integrals, the derivatives involved in the gradient operator, etc).

At each frequency, Eq. (13) is a linear system of N equations with N unknowns, where N is the number of nodes of the mesh in $\{\mathbf{k}\}$ space. This system can be solved using the usual techniques (Gauss procedure), thus giving the perturbed distribution function. In practice, the computed quantity is $\delta f_E = \delta f(\mathbf{k},\omega)/\delta E$, represented by a column matrix $[\delta f_E]$ with elements $\delta f(k_i,\theta_j,\omega)/\delta E$ (N elements), which has a real part $[\delta f_E]_{\rm re}$ and an imaginary part $[\delta f_E]_{\rm im}$. By dividing Eq. (10) by δE, and separating the real and imaginary parts, we obtain

$$\begin{aligned} &[A][\delta f_E]_{\rm re} - \omega[I][\delta f_E]_{\rm im} = [g] , \\ &\omega[I][\delta f_E]_{\rm re} + [A][\delta f_E]_{\rm im} = [0] , \end{aligned} \tag{14}$$

where the square matrix $[A]$ represents the discretized operator $[(e\mathbf{E}_S/\hbar)\cdot\nabla_{\mathbf{k}} - C]$, the column matrix $[g]$ represents the discretized vector $(e/\hbar)\nabla_{\mathbf{k}} f_S(\mathbf{k})$, $[I]$ is the identity matrix. From Eq. (14), one readily obtains

$$\begin{aligned} &[\delta f_E]_{\rm re} = [A]([A]^2 + \omega^2[I])^{-1}[g] , \\ &[\delta f_E]_{\rm im} = -\omega([A]^2 + \omega^2[I])^{-1}[g] . \end{aligned} \tag{15}$$

The unknowns on the left-hand side of Eq. (15) are easily obtained using standard numerical techniques.

In practice, one is generally interested in the longitudinal ac differential mobility, which means $\delta\mathbf{E} \| \mathbf{E}_S$. In addition, $\mathbf{E}_S$ is usually taken along a symmetry axis of the semiconductor crystal; then $\mathbf{v}_S \| \mathbf{E}_S \| \delta\mathbf{v}(\omega)$, and the longitudinal mobility $\mu_{\|}(\omega,\mathbf{E}_S)$ is a scalar quantity, hence only the complex value $\delta v(\omega)$ of $\delta\mathbf{v}(\omega)$ has to be calculated. The quantities of interest are then scalars E_S and δE which are the magnitude of $\mathbf{E}_S$ and $\delta\mathbf{E}$, and the complex quantities $\delta v(\omega)$ and $\mu_{\|}(\omega,E_S)$.

IV. IMPULSE-RESPONSE METHOD

A. Definitions

As is well known from the signal theory for linear systems, working in the frequency or the time domain is a matter of convenience, since the sinusoidal response is the Fourier transform of the impulse response. From a practical point of view, however, one domain can often better facilities of calculations. Therefore, in the following we exploit the time domain approach.

To this purpose, let us assume that the perturbation in Eq. (7) is an impulsed electric field:

$$\delta\mathbf{E}_{\rm imp}(t) = \delta\mathbf{E}\delta(t) , \tag{16}$$

where $\delta(t)$ is the Dirac function. The response is then $\delta f_{\rm imp}(\mathbf{k},t)$ given by Eq. (7):

$$\frac{\partial}{\partial t}\delta f_{\rm imp}(\mathbf{k},t) + \frac{e\mathbf{E}_S}{\hbar}\cdot\nabla_{\mathbf{k}}\delta f_{\rm imp}(\mathbf{k},t) - C\delta f_{\rm imp}(\mathbf{k},t) = -\frac{e\delta\mathbf{E}\delta(t)}{\hbar}\cdot\nabla_{\mathbf{k}} f_S(\mathbf{k}) . \tag{17}$$

From the Fourier transform of the Dirac function, Eq. (16) can be written as

$$\delta E_{\rm imp}(t) = \int_{-\infty}^{+\infty} \delta E \exp(i\omega t)\, d\nu , \tag{18}$$

where $\nu = \omega/2\pi$. Since Eq. (7) is linear with time, Eq. (18) shows that

$$\delta f_{\rm imp}(\mathbf{k},t) = \int_{-\infty}^{+\infty} \delta f(\mathbf{k},\omega)\exp(i\omega t)\, d\nu , \tag{19}$$

where $\delta f(\mathbf{k},\omega)$ is given by Eq. (9). According to Eq. (8), the impulse response of the velocity $\delta\mathbf{v}_{\rm imp}(t)$ is given by

$$\delta\mathbf{v}_{\rm imp}(t) = \left[\int \mathbf{v}(\mathbf{k})\delta f_{\rm imp}(\mathbf{k},t)\, d^3k\right]\left[\int f_S(\mathbf{k})\, d^3k\right]^{-1} ; \tag{20}$$

that is, according to Eq. (19),

$$\delta\mathbf{v}_{\rm imp}(t) = \int_{-\infty}^{+\infty} \delta\mathbf{v}(\omega)\exp(i\omega t)\, d\nu . \tag{21}$$

This result is standard since $\delta\mathbf{v}$ is linear with δf, and δf is related to $\delta\mathbf{E}$ through a linear operator [see Eq. (7)]. Equation (21) shows that $\delta\mathbf{v}(\omega)$ is the Fourier transform of $\delta\mathbf{v}_{\rm imp}(t)$, hence

$$\delta\mathbf{v}(\omega) = \int_{-\infty}^{+\infty} \delta\mathbf{v}_{\rm imp}(t)\exp(-i\omega t)\, dt . \tag{22}$$

B. Calculations

Now we apply a steplike electric-field perturbation $\delta\mathbf{E}_{\rm step}(t)$, given by

$$\delta\mathbf{E}_{\rm step}(t) = \delta\mathbf{E}u(t) , \tag{23}$$

where $u(t)$ is the step function $u(t)=1$ if $t \geq 0$ and $u(t)=0$ if $t<0$. The step distribution response $\delta f_{\rm step}(\mathbf{k},t)$ is then, from Eq. (7)

$$\frac{\partial}{\partial t}\delta f_{\rm step}(\mathbf{k},t) + \frac{e\mathbf{E}_S}{\hbar}\cdot\nabla_{\mathbf{k}}\delta f_{\rm step}(\mathbf{k},t) - C\delta f_{\rm step}(\mathbf{k},t) = -\frac{e\delta\mathbf{E}u(t)}{\hbar}\cdot\nabla_{\mathbf{k}} f_S(\mathbf{k}) , \tag{24}$$

and the step velocity response $\delta\mathbf{v}_{\rm step}(t)$ is given by

$$\delta\mathbf{v}_{\rm step}(t) = \left[\int \mathbf{v}(\mathbf{k})\delta f_{\rm step}(\mathbf{k},t)\, d^3k\right]\left[\int f_S(\mathbf{k})\, d^3k\right]^{-1} . \tag{25}$$

The partial derivative of Eq. (24) with respect to time gives

$$\frac{\partial}{\partial t}\frac{\partial\delta f_{\rm step}(\mathbf{k},t)}{\partial t} + \frac{e\mathbf{E}_S}{\hbar}\cdot\nabla_{\mathbf{k}}\frac{\partial\delta f_{\rm step}(\mathbf{k},t)}{\partial t} - C\frac{\partial\delta f_{\rm step}(\mathbf{k},t)}{\partial t} = -\frac{e\delta\mathbf{E}\delta(t)}{\hbar}\cdot\nabla_{\mathbf{k}} f_S(\mathbf{k}) . \tag{26}$$

Comparison of Eqs. (26) and (17) shows that

$$\frac{\partial\delta f_{\rm step}(\mathbf{k},t)}{\partial t} = \delta f_{\rm imp}(\mathbf{k},t) . \tag{27}$$

To obtain the transient distribution function $\delta f_{\text{step}}(\mathbf{k},t)$, we first solve (using a direct method[16,31]) the transient BE [Eq. (1)] in the constant field E_S, so calculating $f(\mathbf{k},t)$ and $f_S(\mathbf{k})$ in the long-time limit $t=t_S$, where t_S is of the order of 3 ps. Then we solve the transient BE in a constant field $E_S+\delta E$, with the initial distribution equal to $f_S(\mathbf{k})$, thus evaluating the transient $f(\mathbf{k},t)$. The step distribution response is then calculated by difference as $\delta f_{\text{step}}(\mathbf{k},t)=f(\mathbf{k},t)-f_S(\mathbf{k})$. In practice, to save computation time, an original acceleration technique has been used.[32]

Taking into account Eq. (27), and by comparison with Eq. (20), the derivative of Eq. (25) with respect to time gives

$$\frac{d\delta v_{\text{step}}(t)}{dt}=\delta v_{\text{imp}}(t) \ . \tag{28}$$

Hence Eq. (22) writes

$$\delta \mathbf{v}(\omega)=\int_{-\infty}^{+\infty}\frac{d\delta \mathbf{v}_{\text{step}}(t)}{dt}\exp(-i\omega t)dt \ . \tag{29}$$

Equation (29) provides a second method for obtaining the ac longitudinal mobility. Once the steady state in the dc field E_S is calculated, a constant electric-field perturbation δE is superimposed on E_S, and $\delta f_{\text{step}}(\mathbf{k},t)$ is computed. The small-signal velocity response $\delta \mathbf{v}_{\text{step}}(t)$ is computed using Eq. (25), and the small-signal velocity response $\delta \mathbf{v}_{\text{imp}}(t)$ using Eq. (28). Its Fourier transform gives $\delta v(\omega)$ [see Eq. (29)]. Finally the longitudinal mobility in the field E_S is given by

$$\mu\|(\omega,E_S)=\delta v(\omega)/\delta E \ . \tag{30}$$

V. RESULTS

The above procedures are used to calculate the small-signal response characteristics of holes in Si at $T=300$ K. The microscopic model is based on a single spherical nonparabolic band, and considers scattering with acoustic and nonpolar optical-phonon mechanisms as developed in Ref. 31. The stationary distribution function is computed using a matrix method previously described[17,18].

Figures 1–3 show a three-dimensional (3D) view of the perturbation of the distribution function obtained with the methods illustrated in previous sections. Figures 1 and 2 refer to the real and imaginary parts of the perturbation of the distribution function $\delta f(k,\theta,\omega)$ calculated using the harmonic-response method at frequency $\nu=\omega/2\pi=5\times10^{11}$ Hz and $E_S=10$ kV/cm. The perturbing field δE is taken equal to 1 V/cm. Each radial curve gives the variation of $\delta f(k,\theta,\omega)$ at a given value of the angle θ. To provide better evidence of the negative contributions, different perspectives have been used. In analogy with the Drude model for the ac conductivity, the real part describes the dissipative contribution which is in phase with the field while the imaginary part describes the optical contribution which is in quadrature with the field.

Figures 3 show the time dependence of the perturbation of the distribution function $\delta f_{\text{step}}(k,\theta,t)$ calculated using the impulse-response method in a constant field $E_S+\delta E$, with $E_S=10$ kV/cm and $\delta E=0.1E_S$. At time $t=0$, when δE is applied, the distribution function is $f_S(\mathbf{k})$ and Figs. 3(a)–3(e) show the transient response. We remark that at times shorter than the collision time the perturbation is more pronounced; for longer times it extends over many momentum states, so that a magnification of a factor 10 is used to make still visible the perturbation at times longer than 1 ps.

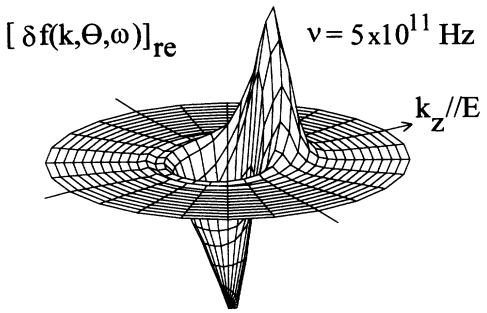

FIG. 1. 3D representation of the real part of the perturbation of the distribution function $[\delta f(k,\theta,\omega)]_{\text{re}}$ (harmonic-response method), in arbitrary scales, at frequency $\nu=\omega/2\pi=5\times10^{11}$ Hz, for holes in Si, $T=300$ K, $E_S=10$ kV/cm, corresponding to a perturbing field $\delta E=1$ V/cm. Each radial curve gives the variation of δf for a given value of the angle θ between $\mathbf{k}$ and $\mathbf{E}$, and each circle corresponds to one value of k (constant energy).

Figure 4 shows the time dependence of the velocity response $\delta \mathbf{v}_{\text{step}}(t)$ at various electric-field strengths. The perturbing field δE is taken equal to 1 V/m in the case $E_S=0$, and equal to $0.1E_S$ in all other cases. By assuming that the response is linear for this small perturbation, the results are normalized to 1 V/m [dividing $\delta \mathbf{v}_{\text{step}}(t)$ by $\delta E/(1\,\text{V/m})$]. At electric fields higher than 5 kV/cm an

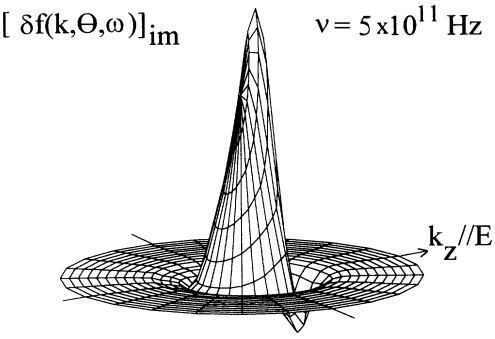

FIG. 2. 3D representation of the imaginary part of the perturbation of the distribution function $[\delta f(k,\theta,\omega)]_{\text{im}}$ (harmonic-response method), in arbitrary scales, at frequency $\nu=\omega/2\pi=5\times10^{11}$ Hz, for holes in Si, $T=300$ K, $E_S=10$ kV/cm, corresponding to a perturbing field $\delta E=1$ V/cm. Each radial curve gives the variation of δf for a given value of the angle θ between $\mathbf{k}$ and $\mathbf{E}$, and each circle corresponds to one value of k (constant energy).

overshoot of the response is clearly evidenced. The steady-state value of $\delta v_{step}(t)$ is greater at low electric field, due to the sublinear slope of the velocity-field curve at increasing electric fields.

Figure 5 shows the velocity-response function $\delta v_{imp}(t)$ versus time, taken as the derivatives of the curves of Fig. 4. At time $t=0$, all curves have practically the same value of $\delta v_{imp}(t=0)=[d\delta v_{step}(t)/dt]_{t=0}=e\delta E/m^*$, where m^* is the effective mass. This is due to the fact that all the carriers are initially accelerated by the perturbing field δE without being scattered. The small changes in $\delta v_{imp}(t=0)$ are due to the nonparabolicity of the band: with increasing values of the electric field, carriers are on average located higher in the band, hence their "average" effective mass m^* slightly increases, so that $\delta v_{imp}(t=0)$ slightly decreases. At zero and low elec-

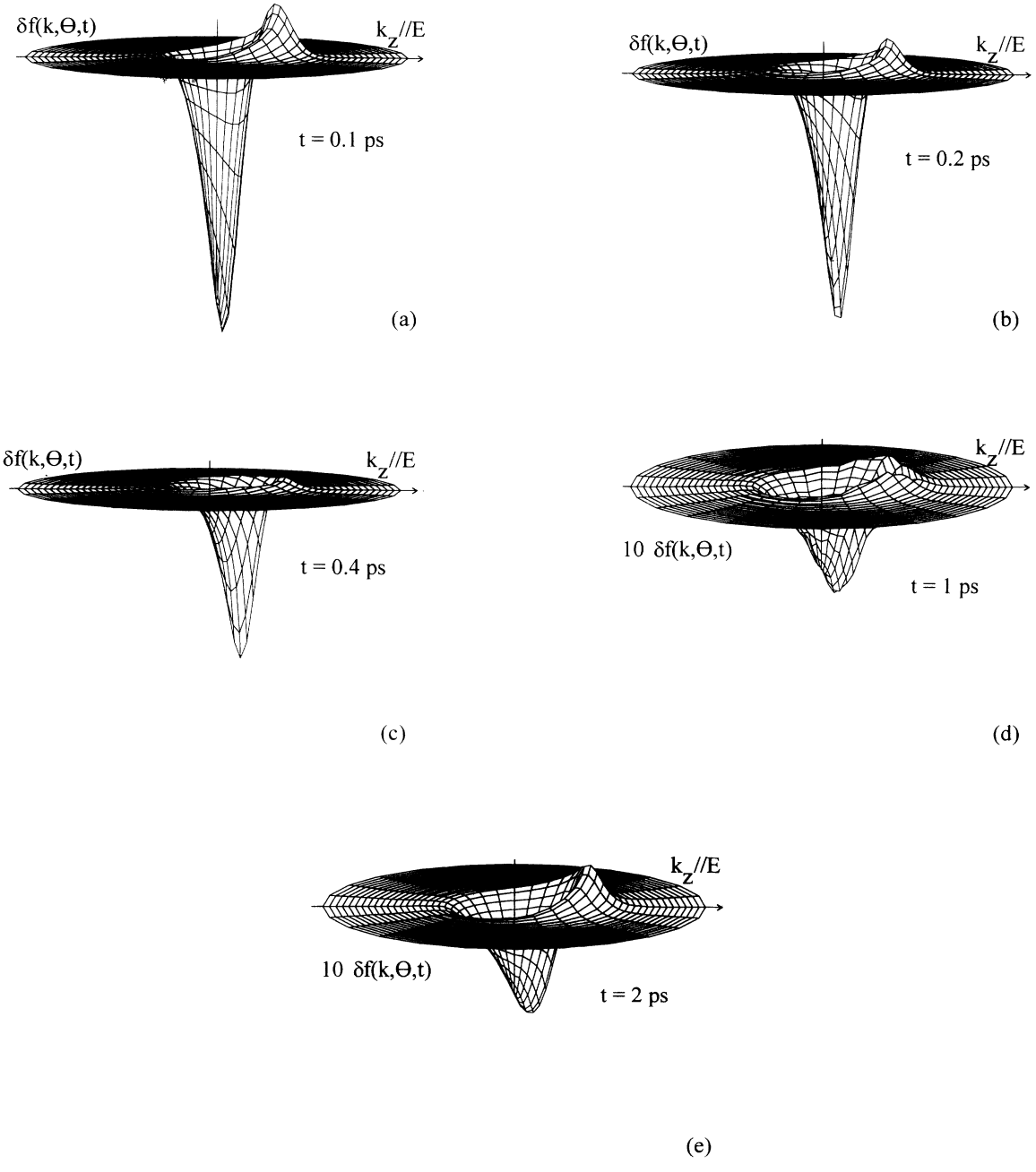

FIG. 3. 3D representation of the perturbation of the distribution function $\delta f_{step}(k,\theta t,)$ (impulse-response method), in arbitrary scales, for holes in Si, $T=300$ K, $E_S=10$ kV/cm, corresponding to a perturbing field $\delta E=1$ kV/cm. At the initial time $t=0$ the system is in a stationary regime at the considered electric field E_S. (a) $t=0.1$ ps, (b) $t=0.2$ ps, (c) $t=0.4$ ps, (d) $t=1$ ps, and (e) $t=2$ ps (new stationary regime at field $E_S+\delta E$).

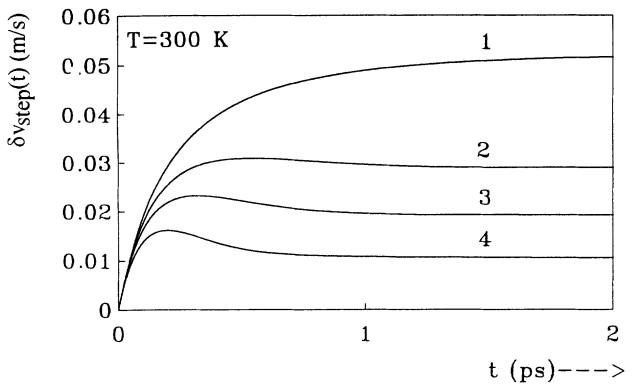

FIG. 4. Scaled transient response of the drift velocity $\delta v_{step}(t)=[v(t)-v_s]\,(1V/m)/\delta E$, when a field step δE is introduced at time $t=0$. At the initial time the system is in a stationary regime at the considered electric field E_S (mean velocity v_S). Calculations refer to holes in Si with $T=300$ K, $\delta E=1$ V/cm for $E_S=0$, and $\delta E=0.1E_S$ otherwise. (1) $E_S=0$, (2) $E_S=5$ kV/cm, (3) $E_S=10$ kV/cm, and (4) $E_S=20$ kV/cm.

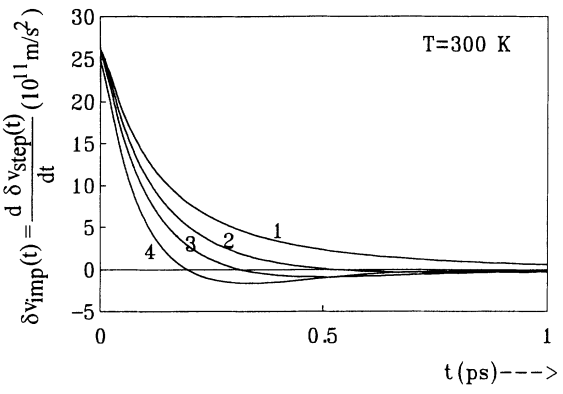

FIG. 5. Time derivative of the transient response of the drift velocity $\delta v_{imp}(t)=d(\delta v_{step}(t))/dt$. Calculations refer to holes in Si with $T=300$ K, $\delta E=1$ V/cm for $E_S=0$, and $\delta E=0.1E_S$ otherwise. (1) $E_S=0$, (2) $E_S=5$ kV/cm, (3) $E_S=10$ kV/cm, and (4) $E_S=20$ kV/cm.

tric fields, the shape of the velocity-response function is practically exponential, with a characteristic time constant which corresponds to momentum relaxation. At higher fields the shape becomes more complicated by exhibiting a negative part which is understood as follows.[33,34] At the initial stage of the velocity relaxation, carriers obtain extra velocity (see Fig. 4), since their initial momentum relaxation time τ_p is somewhat longer than that in the new steady state. Then, the energy relaxation affects τ_p (i.e., τ_p becomes shorter) and this extra velocity is lost. Therefore, the energy relaxation is responsible for the negative contribution of the velocity-response function.

The harmonic- and impulse-response methods are further used to calculate the differential mobility spectrum which is reported in Figs. 6 and 7.

Within the first method (reported by circles in different figures), the computed perturbation $\delta f(k,\theta,\omega)$ is substituted into Eq. (11), thus giving the perturbed complex velocity, and the complex mobility after division by δE [Eq. (12)]. Within the second method (reported by continuous lines in different figures), the mobility is given by Eq. (30). The circles in figures 6(a)–6(f) show the real part μ_r and the imaginary part μ_i of the ac mobility computed as described above. The circles in Figs. 7(a)–7(f) show the modulus $|\mu|$ and the argument $\varphi=\arg\mu$ for the ac mobility, in the same conditions as for Figs. 6(a)–6(f), respectively. The solid lines in Figs. 6(a)–6(f) show the real part μ_r and imaginary part μ_i of the ac mobility computed as the Fourier transform of the step response for various values of the applied electric field. The solid lines on Figs. 7(a)–7(f) show the modulus $|\mu|$ and the argument $\varphi=\arg\mu$ for the ac mobility, in the same conditions as for Fig. 6(a)–6(f), respectively. As can be seen from Figs. 6 and 7, the agreement between the two techniques developed in this paper for obtaining the ac mobility is excellent, thus validating the present approach.

In particular, from Figs. 6 and 7 a deviation from the simple Drude slope of μ_r and μ_i is evidenced. This peculiarity is explained as follows. At zero and low dc electric fields, the time dependence of the step velocity response $\delta v_{step}(t)$ is near exponential (see Fig. 4), hence the impulse velocity response $\delta v_{imp}(t)$ decreases monotonously with increasing time μ_r, $|\mu|$, and φ decrease with increasing frequency, and μ_i is negative. The characteristic relaxation time involved is then the momentum relaxation time.

At higher fields, the energy relaxation time begins to play a role. This results in a transient velocity overshoot for $\delta v_{step}(t)$ and in a negative value of $\delta v_{imp}(t)$, which, as seen in Figs. 6 and 7, corresponds to a bump in μ_r, $|\mu|$, and φ. With increasing electric field, these quantities increase in low-frequency region, which implies a positive value of μ_i, then decrease resulting in a negative value of μ_i.

Now, from Eq. (22), taking into account that the impulse response starts at $t=0$, one obtains

$$\delta v(\omega)_I=-\int_0^\infty \sin(\omega t)\delta v_{imp}(t)dt$$
$$=-\sum_{n=0}^{\infty}\int_{nT}^{(n+1)T}\sin(\omega t')\delta v_{imp}(t')dt' , \qquad (31)$$

where $T=\omega/2\pi$. Cutting the period T in two half parts, then setting $t'=t$ in the first half period and $t'=t+T/2$ in the second half period gives, taking into account the symmetry of the sin function,

$$(\delta v(\omega))_I=-\sum_{n=0}^{\infty}\int_{nT}^{nT+T/2}\sin(\omega t')[\delta v_{imp}(t')-\delta v_{imp}(t'+T/2)]dt' . \qquad (32)$$

Equation (32) shows that, if $\delta v_{imp}(t)$ is a monotonously decreasing function of time, the integral in each time interval is positive or null, then $(\delta v(\omega))_I \leq 0$. $(\delta v(\omega))_I$ tends toward zero only if ω tends toward zero or infinity. Therefore we see that at intermediate frequencies $(\delta v(\omega))_I = 0$ can occur only if, after decreasing, $\delta v_{imp}(t)$ increases, which means that $\delta v_{imp}(t)$ has a minimum value. This occurs in particular when $\delta v_{imp}(t)$ becomes negative then increases; that is, the step velocity $\delta v_{step}(t)$ exhibits an overshoot.

We have thus established that the step velocity overshoot, the negative impulse velocity, and the vanish-

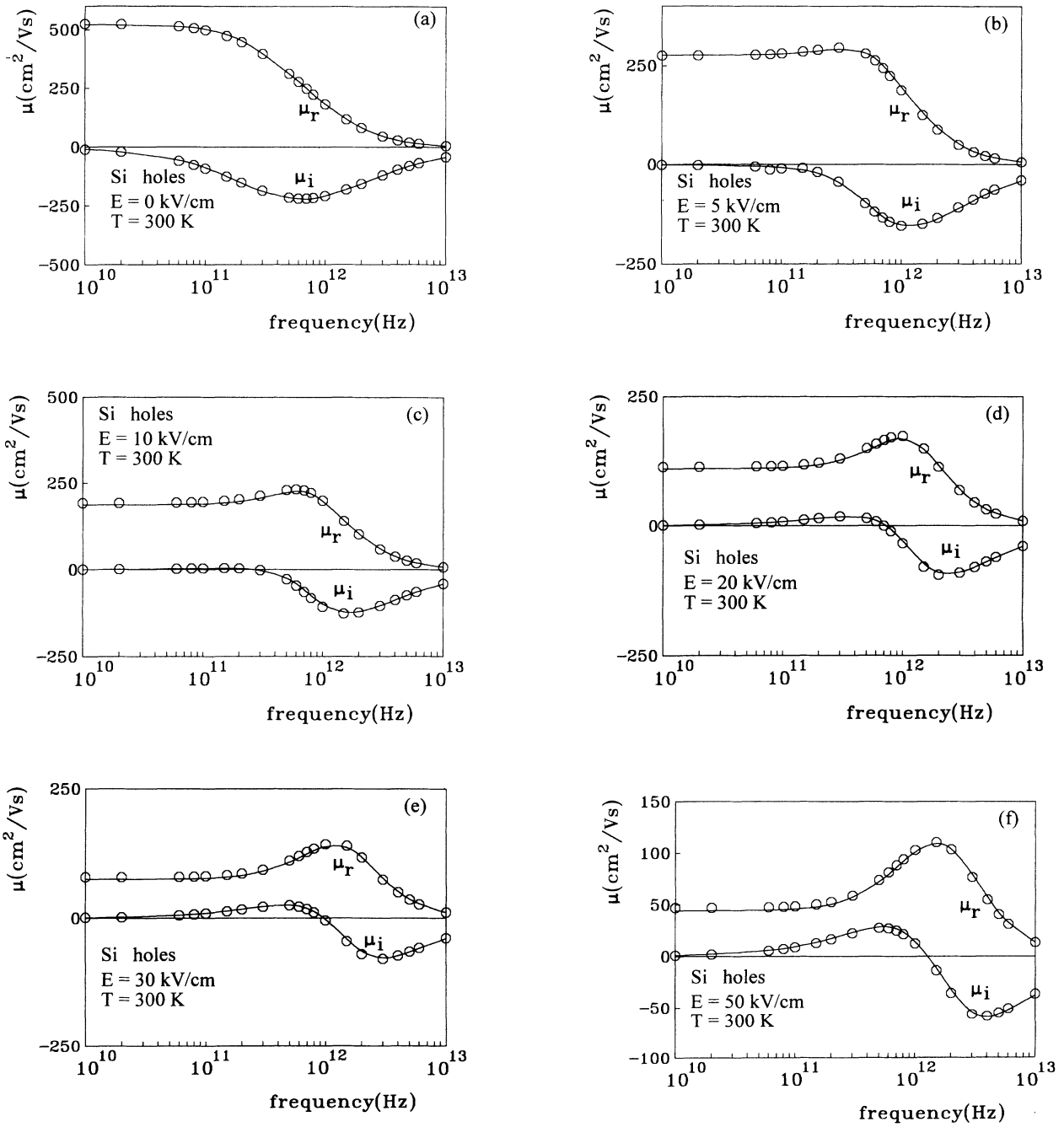

FIG. 6. Real part μ_r and imaginary part μ_i of the ac mobility for holes in Si at various values of the applied dc electric field E_S. (a) $E_S = 0$ (ohmic mobility), (b) $E_S = 5$ kV/cm, (c) $E_S = 10$ kV/cm, (d) $E_S = 20$ kV/cm, (e) $E_S = 30$ kV/cm, and (f) $E_S = 50$ kV/cm. Circles: ac mobility derived from the computation of the perturbed distribution function corresponding to a perturbing electric field $\delta E = 1$ V/cm superimposed on the dc field E_S (harmonic-response method). Solid line: ac mobility derived from the velocity response to a step electric field δE superimposed on the dc field E_S (impulse-response method). $\delta E = 1$ V/m in case (a) and $0.1 E_S$ in all other cases.

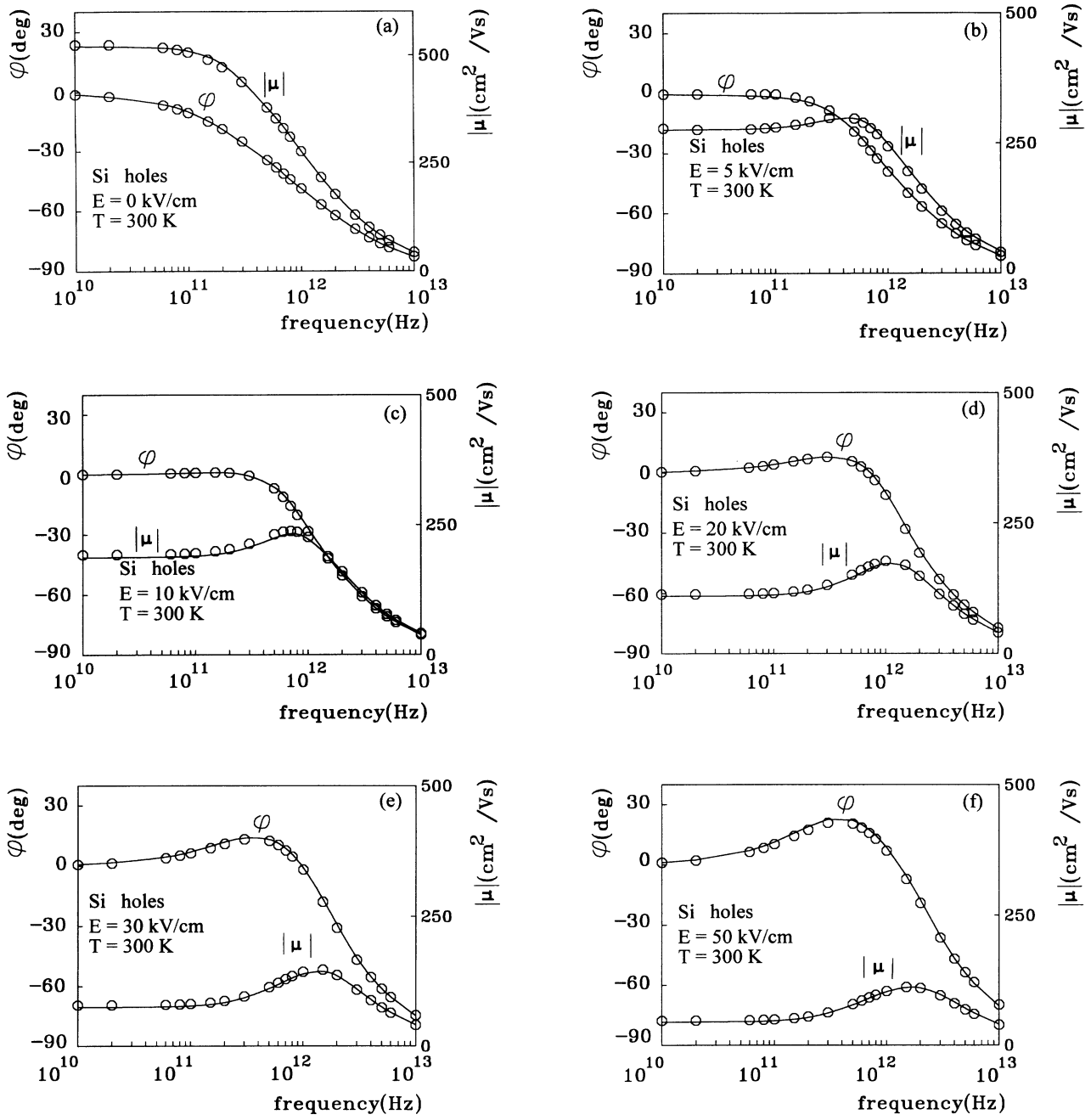

FIG. 7. Modulus $|\mu|$ and argument $\varphi = \arg\mu$ of the ac mobility for holes in Si at various values of the applied dc electric field E_S. (a) $E_S = 0$ (ohmic mobility), (b) $E_S = 5$ kV/cm, (c) $E_S = 10$ kV/cm, (d) $E_S = 20$ kV/cm, (e) $E_S = 30$ kV/cm, and (f) $E_S = 50$ kV/cm. Circles: ac mobility derived from the computation of the perturbed distribution function corresponding to a perturbing electric field $\delta E = 1$ V/cm superimposed on the dc field E_S (harmonic-response method). Solid line: ac mobility derived from the velocity response to a step electric field δE superimposed on the dc field E_S (impulse-response method). $\delta E = 1$ V/m in case (a), and $0.1E_S$ in all other cases.

ing imaginary part of the mobility all describe the same microscopic phenomena.

VI. CONCLUSION

We here have presented two methods for calculating the small-signal response around the dc bias in bulk semiconductors, using direct numerical resolutions of the perturbed Boltzmann equation.

The first method operates in the frequency domain. An ac sinusoidal electric-field perturbation is superimposed on the dc field. This produces an ac perturbation of the distribution function $\delta f(\mathbf{k},\omega)$, which is computed at each frequency. After multiplication by the velocity $\mathbf{v}(\mathbf{k})$ and

integration in $\{\mathbf{k}\}$ space, one obtains the ac longitudinal mobility $\mu_{\parallel}(\omega)$ versus frequency.

The second method operates in the time domain. A step electric-field perturbation is superimposed at time $t=0$ on the dc field. This produces a time-dependent perturbation $\delta f(\mathbf{k},t)$ and $\delta v_{\text{step}}(t)$ of the distribution function and of the average velocity. The Fourier transform of the time derivative of $\delta v_{\text{step}}(t)$ gives the ac longitudinal mobility $\mu_{\parallel}(\omega)$.

Both methods have been validated for the case of holes in silicon, and proven to give exactly the same results. Comparing the harmonic and impulse-response methods, we can state the following.

(i) Both methods are deterministic and therefore overcome the difficulties of the stochastic methods (such as Monte Carlo simulations) in calculating with high accuracy transport parameters on a hydrodynamic time scale.

(ii) The former can use very small perturbations of the electric field, while it is necessary to take a few percent of electric field in the impulse-response method.

(iii) The advantage of the last method is to use directly the code developed for solving the transient Boltzmann equation (without modification).

(iv) The former method requires solving the perturbed Boltzmann equation for each frequency of interest, while the latter gives the whole mobility spectrum by a simple Fourier transform of the velocity-response function.

The calculation of the differential mobility spectrum for holes in silicon shows that at increasing dc fields, a bump in the real part of the ac mobility is observed at very high frequencies ($\gg 1000$ GHz). This bump is associated with a negative impulse response of the velocity, corresponding to a small-signal step velocity overshoot due to the rapid increase of the scattering rates as a function of the carrier energy.

ACKNOWLEDGMENTS

This work is supported by the Commission of European Community (CEC) in the framework of the Human capital and Mobility program, by the French Groupement Circuit Intégrés Silicium (GCIS), by the Italian Consiglio Nazionale delle Ricerche (CNR), by a Soros Foundation Grant awarded by the American Physical Society, and by the Italian Ministero della Università e della Ricerca Scientifica e Tecnologica (MURST).

*On leave from Dipartimento di Fisica, Università di Modena, Via Campi 213/A, 41100 Modena, Italy.

[1]P. J. Price, Semicond. Semimet. **14**, 249 (1979).

[2]R. W. Hockney and J. W. Eastwood, *Computer Simulation Using Particles* (McGraw-Hill, New York, 1981).

[3]C. Jacoboni and L. Reggiani, Rev. Mod. Phys. **55**, 645 (1983).

[4]C. Jacoboni and P. Lugli, *The Monte Carlo Method for Semiconductor Device Simulation,* edited by S. Selberherr, Springer Series in Computational Micro Electronics (Springer, Berlin, 1989).

[5]M. V. Fischetti and S. E. Laux, Phys. Rev. B **38**, 9721 (1988).

[6]*Supercomputer Simulation of Semiconductor Devices,* edited by M. Shur and T. A. Fjeldy (North-Holland, Amsterdam, 1991).

[7]P. J. Price, J. Appl. Phys. **54**, 3616 (1983).

[8]E. Starikov and P. Shiktorov, Fiz. Tekh. Polvprovodn. **22**, 72 (1988) [Sov. Phys. Semicond. **22**, 45 (1988)].

[9]F. Rossi, P. Poli, and C. Jacoboni, Semicond. Sci. Technol. **7**, 1017 (1992).

[10]A. Das and M. S. Lundstrom, Solid State Electron. **33**, 1299 (1990).

[11]H. Lin, N. Goldsman, and I. D. Mayergoyz, Solid State Electron. **35**, 769 (1992).

[12]A. Gnudi, D. Ventura, G. Baccarani, and F. Oden, Solid State Electron. **36**, 575 (1993).

[13]F. J. Mustieles and F. Delaurens, Solid State Electron. **36**, 857 (1993).

[14]H. D. Rees, J. Res. Dev. **13**, 537 (1969).

[15]M. A. Stettler and M. S. Lundstrom, Appl. Phys. Lett. **60**, 2908 (1992).

[16]P. A. Lebwohl and P. M. Marcus, Solid State Commun. **9**, 1671 (1971).

[17]J. P. Aubert, J. C. Vaissiere, and J. P. Nougier, J. Appl. Phys. **56**, 1128, (1984).

[18]J. C. Vaissiere, J. P. Nougier, M. Fadel, L. Hlou, and P. Kocevar, Phys. Rev. B **46**, 13 082 (1992).

[19]J. P. Nougier, and M. Rolland, Phys. Rev. B **8**, 5728 (1973).

[20]M. Fadel, M. Rieger, J. C. Vaissiere, J. P. Nougier, and P. Kocevar, Solid-State Electron. **32**, 1229 (1989).

[21]J. P. Nougier, *III-V Microelectronics,* edited by J. P. Nougier (North-Holland, Amsterdam, 1991), pp. 1–56.

[22]J. C. Mc Grooddy and P. Gueret, Solid-State Electron. **14**, 1279 (1971).

[23]B. J. Vinter, J. Phys. C **7**, 2187 (1974).

[24]Yu. Pozhela and A. Reklaitis, Fiz. Tekh. Poluprodn. **13**, 1127 (1979) [Sov. Phys. Semicond. **13**, 660 (1979)].

[25]P. J. Price, J. Appl. Phys. **53**, 8805 (1982).

[26]P. Dollfus, S. Galdin, C. Brisset, and P. Hesto, J. Phys. III (France) **3**, 1713 (1993).

[27]E. V. Starikov and P. N. Shiktorov, Lietuvos Fizikos Rinkinys **32**, 471 (1992).

[28]J. P. Nougier, Physica **64**, 209 (1973).

[29]J. P. Nougier, in *Proceedings of the 6th International Conference on Noise in Physical Systems,* edited by P. H. E. Meijer, R. D. Mountain, and R. J. Soulen (National Bureau of Standards, Washington, 1981), pp. 42–46.

[30]J. P. Nougier, L. Hlou, and J. C. Vaissiere, in *Proceedings of the 8th International Conference on Noise in Physical Systems,* edited by P. H. Handel and A. L. Chung (AIP, New York, 1993), pp. 57-60.

[31]J. C. Vaissière, Thèse de Doctorat ès Sciences, Université Montpellier II (France), 1986 (available upon request).

[32]L. Hlou, Thése de Doctorat, Université Montpellier II (France), 1993 (available upon request).

[33]T. Kuhn, L. Reggiani, and L. Varani, Phys. Rev. B **42**, 11 133 (1990).

[34]V. Gruzhinskis, E. Starikov, P. Shiktorov, L. Reggiani, M. Saraniti, and L. Varani, Semicond. Sci. Technol. **8**, 1283 (1993).

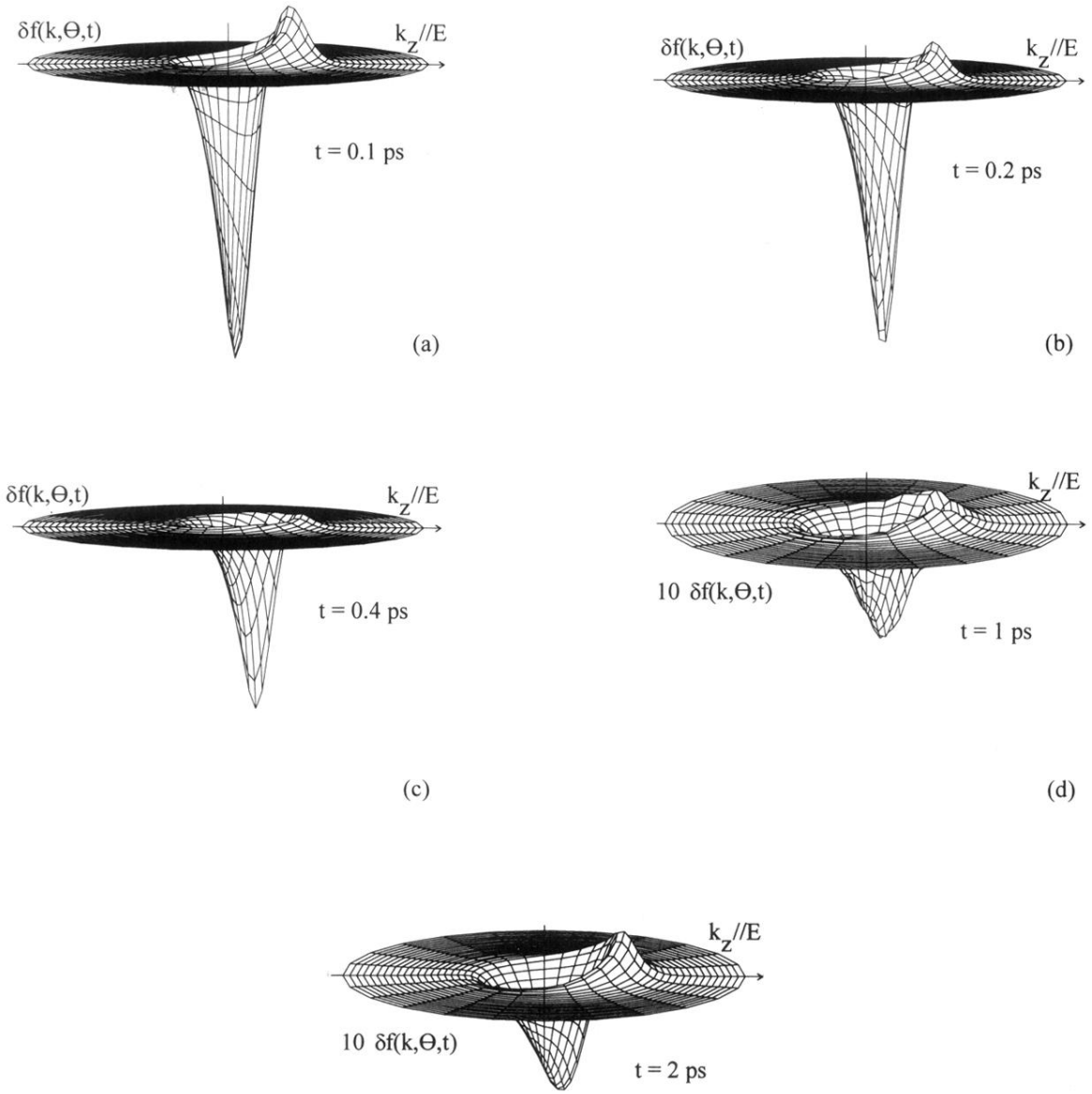

FIG. 3. 3D representation of the perturbation of the distribution function $\delta f_{\text{step}}(k,\theta t,)$ (impulse-response method), in arbitrary scales, for holes in Si, $T=300$ K, $E_S=10$ kV/cm, corresponding to a perturbing field $\delta E=1$ kV/cm. At the initial time $t=0$ the system is in a stationary regime at the considered electric field E_S. (a) $t=0.1$ ps, (b) $t=0.2$ ps, (c) $t=0.4$ ps, (d) $t=1$ ps, and (e) $t=2$ ps (new stationary regime at field $E_S+\delta E$).